



# Automatic Coronary Artery Image Segmentation and Catheter Detection in Angiographic Images

<sup>1</sup>Dr. S.Karthick, <sup>2</sup>Dr.K. Sathiyasekar, <sup>3</sup>Ms.Anuradha Balasubramaniam, <sup>4</sup>Dr.S.Karthikeyan

<sup>1</sup>\*Assistant Professor/ECE, Erode Sengunthar Engineering College, Erode, Tamil Nadu, India.

<sup>2</sup>Professor/ECE, Prathyusha Engineering College, Chennai, Tamil Nadu, India.

<sup>3</sup>Assistant Professor/ECE, Sri Eshwar College of Engineering, Coimbatore, Tamil Nadu, India.

<sup>4</sup>Professor/ECE, Chaitanya Bharathi Institute of Technology, Proddatur, Andhra Pradesh, India.

<sup>1</sup>researchkarthick@gmail.com, <sup>2</sup>ksathiyasekar@gmail.com,

\*Corresponding Author: <sup>1</sup>Dr. S.Karthick, researchkarthick@gmail.com

## Abstract

Segmentation of coronary arteries in angiography images is a fundamental tool to evaluate arterial diseases and choose proper coronary treatment. The accurate segmentation of coronary arteries has become an important topic for the registration of different modalities, which allows physicians rapid access to different medical imaging information from Computed Tomography (CT) scans or Magnetic Resonance Imaging (MRI). An accurate fully automatic algorithm based on Graph-cuts for vessel centerline extraction, calibre estimation, and catheter detection is proposed. Vesselness, geodesic paths, and a new multiscale edgeness map are combined to customize the Graph-cuts approach to the segmentation of tubular structures, by means of a global optimization of the Graph-cuts energy function. A novel supervised learning methodology that integrates local and contextual information is proposed for automatic catheter detection. Graph cut method is implemented by using Gaussian and Gabor filter and both methods are compared.

4754

**Keywords:** Coronary Artery, Angiographic Image, Image segmentation, Multi Scale Vessel, Quantitative Coronary Angiography, Canny Edge Detection

**DOI Number:**10.14704/nq.2022.20.8.NQ44502

**NeuroQuantology 2022; 20(8): 4754-4765**

## Introduction

Image processing is a physical process used to convert an image signal into a physical image. The image signal can be either digital or analog. The actual output itself can be an actual physical image or the characteristics of an image. The most common type of image processing is photography. In this process, an

image is captured or scans using a camera to create a digital or analog image[1,2]. In order to produce a physical picture, the image is processed using the appropriate technology based on the input source type. In digital photography, the image is stored as a computer file. This file is translated using photographic software to generate an actual image. The



colors, shading, and nuances are all captured at the time the photograph is taken the software translates this information into an image[3]. When creating images using analog photography, the image is burned into a film using a chemical reaction triggered by controlled exposure to light. The image is processed in a darkroom, using special chemicals to create the actual image. This process is decreasing in popularity due to the opening of digital photography, which requires less effort and special training to product images[4,5]. The various basic steps are as follows: Image Acquisition, Image preprocessing, Image segmentation, Image Representation and Description, Image Recognition and Interpretation and Knowledge base.

### Image Acquisition

In the process, the first step in the process is image acquisition that is, to acquire a digital image. It highly requires an imaging sensor and the capability to digitize the signal produced by the sensor. The sensor could be a monochrome or color TV camera that produces an entire image of the problem domain every 1/30 sec. The imaging sensor could also a line-scan camera that produces a single image line at a time. In this case, the object's motion past the line scanner produces two-dimensional image[6]. If the output of the camera or other imaging sensor is not already in digital form, an analog-to-digital converter digitizes it. The nature of the sensor and image it produces are determined by the application.

## Fig 1: The Fundamental steps in digital image processing

### Image Preprocessing

The key function of preprocessing is to improve the image in ways that increase the chances for success of the other processes. Preprocessing typically deals with techniques for enhancing contrast, removing noise, and isolating regions whose texture indicate a likelihood of alphanumeric information.

#### Image Enhancement:

Improve the image quality and brightness. It will be more suitable than the original image for a specific application.

#### Image Restoration:

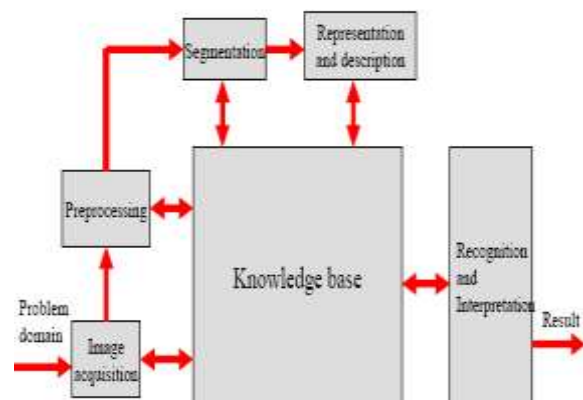
A process that attempts to reconstruct or recover an image that has been degraded using prior knowledge of the degradation concept.

### Image Segmentation

The next stage deals with segmentation. Segmentation partitions an input image into its small constituent parts or objects. It is the fundamental step in every image processing application in biomedical field. In general, autonomous segmentation is one of the most difficult tasks in digital image processing[7,8]. On the one hand, a rugged segmentation procedure brings the process a long way towards the successful solution of an imaging problem. On the other hand, weak or erratic segmentation algorithms almost guarantee eventual failure. In terms of character recognition, the key role of segmentation is to extract individual characters and words from the background.

### Image Representation and Description

The output of the segmentation stage usually is raw pixel data, constituting either the boundary of a region or all the points in the region itself. In either case converting the data to a form suitable for computer processing is necessary. The first decision that must be made, whether the data should be represented as a boundary or as a complete region. Boundary



representation is appropriate when the focus is on external shape characteristics, such as corners and inflections[9]. Regional representation is appropriate when the focus is on internal properties, such as texture or skeletal shape. In some applications, however, these representations coexist[10]. This situation occurs in character recognition applications, which often require algorithms based on boundary shape as well as skeletons and other internal properties.

### **Image Recognition and Interpretation**

Recognition is the process that assigns a label to an object based on the information provided by its descriptors. Interpretation involves assigning meaning to an ensemble of recognized objects.

### **Knowledge Base**

This knowledge may be as simple as detailing regions of an image where the information of interest is known to be located, thus limiting the search that has to be conducted in seeking that information[11,12]. The knowledge base also can be quite complex, such as an interrelated list of all major possible defects in a materials inspection problem or an image database containing high-resolution satellite images of a region in connection with change-detection applications. In addition to guiding the operation of each processing module, the knowledge base also controls the interaction between modules.

### **Coronary Artery Disease (CAD)**

Coronary Artery Disease (CAD) is a complex disease that causes reduced or absent blood flow in one or more of the arteries that encircle and supply the heart[13]. The disease may be focal or diffuse. Apart from rare congenital anomalies, CAD is usually a degenerative disease, uncommon as a clinical problem before the age of 30 years and common by the age of 60 years. One in four people will have a heart attack. The first recognized symptom may be death. The term coronary is derived from crown, referring to the way these arteries sit on the heart. When the heart has inadequate blood supply, pressure may be felt in the chest

that moves to the left arm; one may feel weak, sweaty, or short of breath or nauseated; palpitations may occur; or there may be a sensation of pressure or tightness just in the chest, neck, or arms. Coronary artery disease is the narrowing or blockage of the coronary arteries, usually caused by atherosclerosis. Atherosclerosis is the buildup of cholesterol and fatty deposits (called plaques) on the inner walls of the arteries. These plaques can restrict blood flow to the heart muscle by physically clogging the artery or by causing abnormal artery tone and function[14,15]. Without an adequate blood supply, the heart becomes starved of oxygen and the vital nutrients it needs to work properly. This can cause chest pain called angina. If blood supply to a portion of the heart muscle is cut off entirely, or if the energy demands of the heart become much greater than its blood supply, a heart attack (injury to the heart muscle) may occur.

### **Quantitative Coronary Angiography**

Quantitative Coronary angiography has become an invaluable tool for the interventional cardiologist, providing objective and reproducible measurements of coronary artery dimensions, which can be used to study progression or regression of coronary atherosclerosis, as well as the immediate and long term effects of percutaneous interventions[16]. Quantitative Coronary angiography can be employed in clinical practice during diagnostic coronary angiography, to have an objective and independent parameter for the assessment of stenosis severity as the human eye does not have the resolution capability of software. Usually, visual interpretation of the severity of a coronary stenosis is expressed in intervals of percentage of stenosis while Quantitative Coronary angiography produces a single specific measure for DS, improving the accuracy and reproducibility of the severity assessment. Coronary lesions can be assessed qualitatively and quantitatively, in terms of severity of the lesion itself. The qualitative evaluation is based on the visual estimation of the lesion and it



depends very much on the operator's experience. The quantitative evaluation, based on QCA, allows instead obtaining numeric parameters that are much more independent

from the operator acquiring the images or the one performing the analyses. The coronary parameters of major interest are summarized in the Table 1.

| Parameter                       | Range commonly used | Meaning  |
|---------------------------------|---------------------|--|
| Minimal Luminal Diameter (MLD)  | 0–6.00 mm           | The smallest lumen diameter in the segment of interest   |
| Reference Vessel Diameter (RVD) | 1.5–6.0 mm          | The averaged diameter of the coronary assumed without atherosclerotic disease  |
| Lesion length                   | 0–60.0 mm           | Length of the stenosis as measured by 2 points where the coronary margins change direction, creating a shoulder between the angiographically normal sub segment and the diseased sub segment |
| Acute gain                      | 0–4.0 mm            | Post-procedural MLD – pre-procedural MLD   |
| Late loss (LL)                  | 0.10 to 3.00        | Post-procedural MLD – MLD at follow-up   |
| Diameter Stenosis (DS)          | 0–100%              | (RVD-MLD)/RVD  |
| Binary Restenosis (BR)          | Yes or No           | DS >50% at follow-up coronary angiography in the treated coronary segment  |

**Table 1: Parameters related to Coronary Artery Disease**

### Existing Methodology

Graph cut algorithm is used for centerline, diameter and boundary of vessel estimation and point wise classification using adaboost classifier is used for catheter detection. Graph cut energy functional tailored to the vessel segmentation problem. The novel energy formulation takes into account

- The local vessel appearance, using a vesselness measure
- The local connectivity to other vessel regions, using geodesic paths
- A measure of edginess based on a new multiscale version of the adaptive Canny detector, which allows an accurate vessel boundary detection.

### Preprocessing

#### Gaussian filtering

A Gaussian blur (also known as Gaussian smoothing) is the result of blurring an image by a Gaussian function. It is a widely used effect in graphics software, typically to reduce image

noise and reduce detail[17]. The visual effect of this blurring technique is a smooth blur resembling that of viewing the image through a translucent screen, distinctly different from the bokeh effect produced by an out-of-focus lens or the shadow of an object under usual illumination. Gaussian smoothing is also used as a pre-processing stage in computer vision algorithms in order to enhance image structures at different scales[18]. The Gaussian blur is a type of image-blurring filters that uses a Gaussian function (which also expresses the normal distribution in statistics) for calculating the transformation to apply to each pixel in the image. The equation of a Gaussian function in one dimension is

$$G(x) = \frac{1}{\sqrt{2\pi\sigma^2}} e^{-\frac{x^2}{2\sigma^2}} \quad (1)$$

in two dimensions, it is the product of two such Gaussians, one in each dimension:



$$G(x, y) = \frac{1}{\sqrt{2\pi\sigma^2}} e^{-\frac{x^2+y^2}{2\sigma^2}} \quad (2)$$

where  $x$  is the distance from the origin in the horizontal axis,  $y$  is the distance from the origin in the vertical axis, and  $\sigma$  is the standard deviation of the Gaussian distribution.

### Canny edge detector

#### Stages of the canny algorithm

1. Noise reduction: image is convolved with a Gaussian filter
2. Finding the intensity gradient of the image
  - Intensity gradient is estimated from the smoothed image using simple horizontal and vertical difference operators
  - Gradient direction together with the gradient magnitude then gives an estimated intensity gradient at each point in the image
  - Canny algorithm uses both gradient magnitude and direction in the edge detection.
  - The gradient magnitude and gradient direction are continuous image functions where  $\arg(x, y)$  is the angle (in radians) from the  $x$ -axis to the point  $(x, y)$ .

$$|\text{grad } g(x, y)| = \sqrt{\left(\frac{\partial g}{\partial x}\right)^2 + \left(\frac{\partial g}{\partial y}\right)^2} \quad (3)$$

$$\psi = \text{arg} \left( \frac{\partial g}{\partial x}, \frac{\partial g}{\partial y} \right) \quad (4)$$

- The gradient direction gives the direction of maximal growth of the function, e.g., from black ( $f(i,j)=0$ ) to white ( $f(i,j)=255$ ). The gradient direction and edge direction diagram illustrates:
  - Closed lines are lines of the same brightness.
  - The orientation  $0^\circ$  points east.



**Fig 2: Gradient direction and edge direction**

### Adaboost Classifier

AdaBoost is an algorithm for constructing a "strong" classifier as linear combination of "simple" "weak" classifiers  $h_t(x)$ .

$$f(x) = \sum_{t=1}^T a_t h_t(x) \quad (5)$$

Algorithm based on multi-scale stacked sequential learning, which includes point wise classification method using adaboost classifier and contextual information extracted and refined by stacked classifier. Adaboost is a predictive algorithm for classification and regression. Adaboost is an ensemble learning algorithm that can be used for classification or regression.

### Proposed Methodology

#### Preprocessing Using By Gabor Filter

In image processing, a Gabor filter, is a linear filter used for edge detection. Frequency and orientation representations of Gabor filters are similar to those of the human visual system, and they have been found to be particularly appropriate for texture representation and discrimination. In the spatial domain, a 2D Gabor filter is a Gaussian kernel function modulated by a sinusoidal plane wave. Simple cells in the visual cortex of mammalian brains can be modeled by Gabor functions. Thus, image analysis with Gabor filters is thought to be similar to perception in the human visual system. Its impulse response is defined by a sinusoidal wave multiplied by a Gaussian function [19,20]. Because of the multiplication-convolution property (Convolution theorem), the Fourier transform of a Gabor filter's impulse response is the convolution of the Fourier



transform of the harmonic function and the Fourier transform of the - Gaussian function. The filter has a real and an imaginary component representing orthogonal directions.

The two components may be formed into a complex number or used individually.

Complex

$$g(x, y; \lambda, \psi, \theta, \sigma, \gamma) = \exp\left(-\frac{x'^2 + \gamma^2 y'^2}{2\sigma^2}\right) \exp\left(i\left(2\pi\frac{x'}{\lambda} + \psi\right)\right) - (6)$$

Real

$$g(x, y; \lambda, \psi, \theta, \sigma, \gamma) = \exp\left(-\frac{x'^2 + \gamma^2 y'^2}{2\sigma^2}\right) \cos\left(2\pi\frac{x'}{\lambda} + \psi\right) - (7)$$

Imaginary

$$g(x, y; \lambda, \psi, \theta, \sigma, \gamma) = \exp\left(-\frac{x'^2 + \gamma^2 y'^2}{2\sigma^2}\right) \sin\left(2\pi\frac{x'}{\lambda} + \psi\right) - (8)$$

Where

$$x' = x \cos\theta + y \sin\theta - (9)$$

and

$$y' = -x \sin\theta + y \cos\theta - (10)$$

In this equation,  $\lambda$  represents the wavelength of the sinusoidal factor,  $\theta$  represents the orientation of the normal to the parallel stripes of a Gabor function,  $\psi$  is the phase offset,  $\sigma$  is the sigma/standard deviation of the Gaussian envelope and  $\gamma$  is the spatial aspect ratio, and specifies the ellipticity of the support of the Gabor function[21]. A set of Gabor filters with different frequencies and orientations may be helpful for extracting useful features from an image. Gabor filters have been widely used in pattern analysis applications.

### Bandwidth

The half-response spatial frequency bandwidth  $b$  (in octaves) of a Gabor filter is related to the ratio  $\sigma / \lambda$ , where  $\sigma$  and  $\lambda$  are of the Gaussian factor of the Gabor function and the preferred wavelength, respectively, as follows the

standard deviation: The value of  $\sigma$  cannot be specified directly[22,23]. It can only be changed through the bandwidth  $b$ . The bandwidth value must be specified as a real positive number. Default is 1, in which case  $\sigma$  and  $\lambda$  are connected as follows:  $\sigma = 0.56 \lambda$ . The smaller the bandwidth, then larger  $\sigma$ . The support of the gabor function and the number of visible parallel excitatory and inhibitory stripe zones[24,25]. Gabor filters kernels with values of the bandwidth parameter of 0.5, 1, and 2, from left to right, respectively. The values of the other parameters are as follows: wavelength 10, orientation 0, phase offset 0, and aspect ratio 0.5.

4759

## Results and Discussion

### Graph cut algorithm using Gaussian filter

#### Input Image

The CT angiographic image is taken as input for vessel segmentation, centerline extraction and catheter detection.





**Fig 3: Input image**

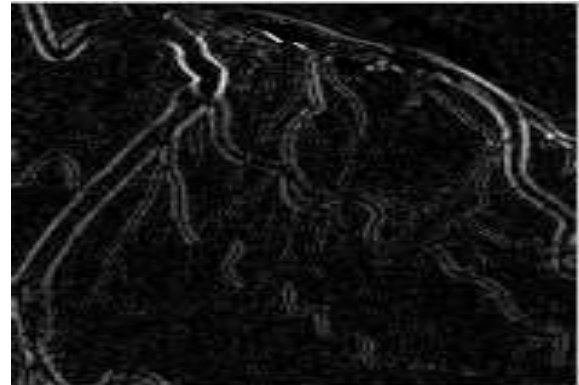


**Fig 5: Vessel and Background separation**

### Output Images Preprocessing

Filters the multidimensional array A with the multidimensional filter H. The array A can be logical or a non sparse numeric array of any class and dimension. The result B has the same size and class as A. Input image is smoothed by Gaussian filter.

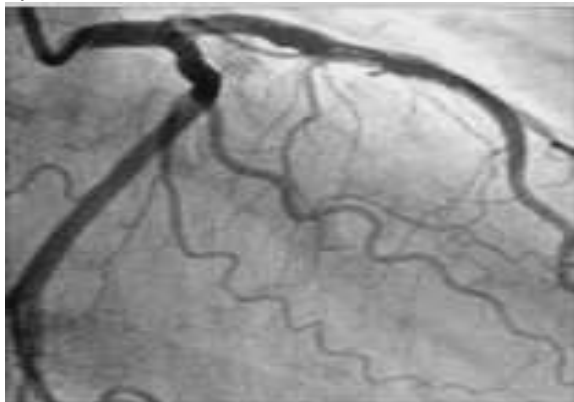


**Fig 4: Filtered image**

### Vessel and Background separation

Calculate graph weights From the filtered output the Vessel structure and Background are separated, since further processing needs only the vessel structure.

### Geodesic distance map

The geodesic distance map contains the distance of each pixel. The distance is the maximum difference of image gradients and the path is computed by Dijkstra's shortest path algorithm. The vessel region is represented in white and the background region is represented in black on Geodesic distance map. The unary term in Graph cut energy formulation is considered from Geodesic distance map.

4760



**Fig 6: Geodesic Distance Map**

### Edgeness map

Canny edge detector algorithm is used to detect the edges. The Boundary term for Graph cut energy formulation is considered from Edgeness map.  $x=0.1:0.1:0.9$ ;



**Fig 7: Edgess map**

### Graph cut Segmentation

By graph cut algorithm, the image is decomposed into N cuts. Each N cuts are taken as vertices and their edges have minimum edge weight. Eigen vectors and Eigen values are taken into account for vessel curvature determination.

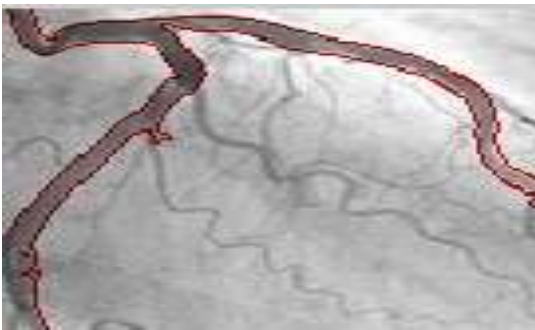


**Fig 8: Graph cut segmentation**

### Centerline Extraction and Catheter Detection

The vessel centerline is extracted by using Non maximal suppression and the non maximal points are joined by Ridge traversal method. The catheter position is detected by distinguishing features on centerline by using adaboost classifier

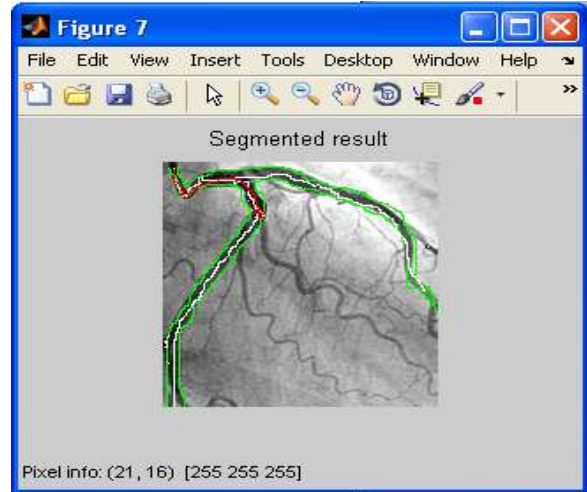


**Fig 8: Center line extraction and Catheter detection**

### Result of Graph Cut Algorithm Using Gabor Filter

Read image

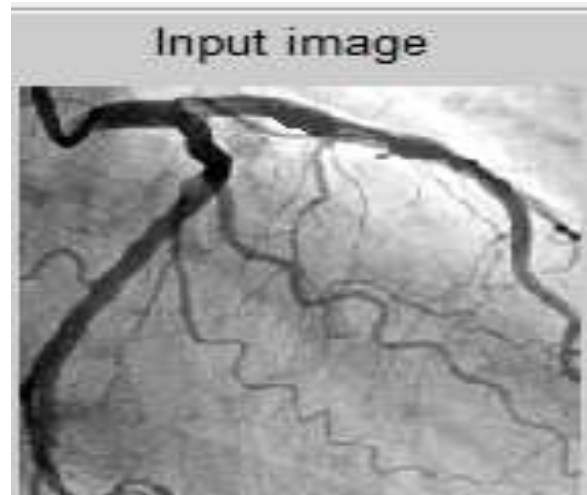


**Fig 9: Input image**

### Color-space Conversion





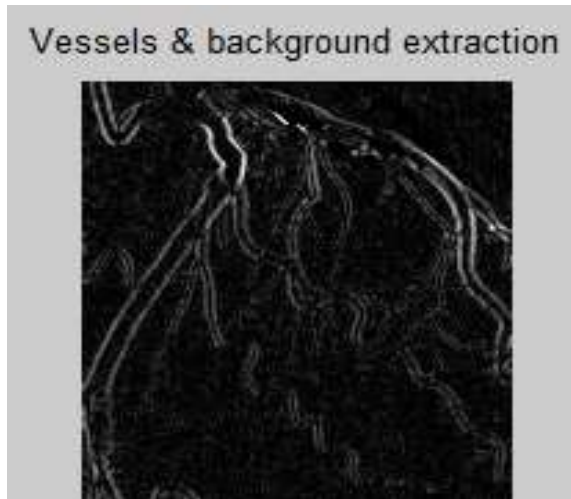


Fig 10: Vessels and Background Extraction

Calculate Graph Weights

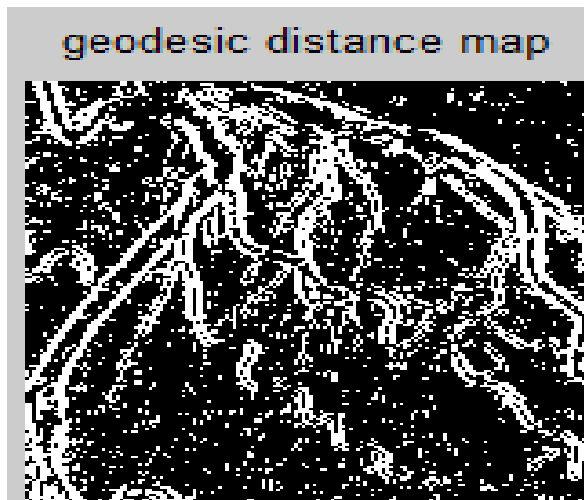


Fig 11: Geodesic Distance Map

Gabor Filter Output

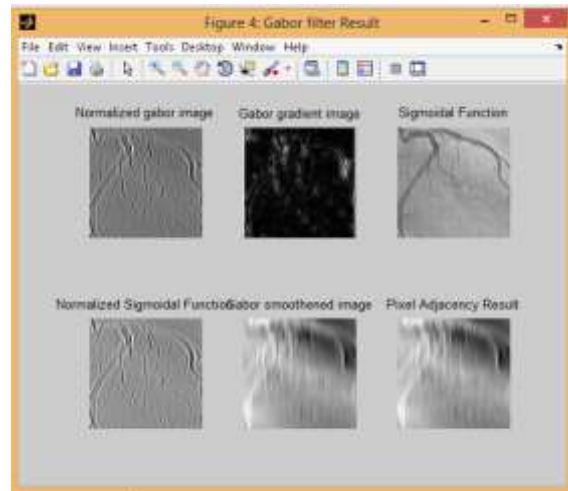


Fig 12: Gabor Filter Output

Adaboost Classifier

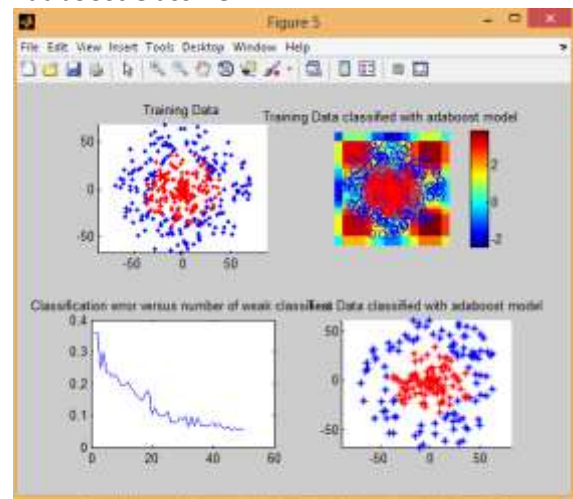


Fig 13: Classified with adaboost model

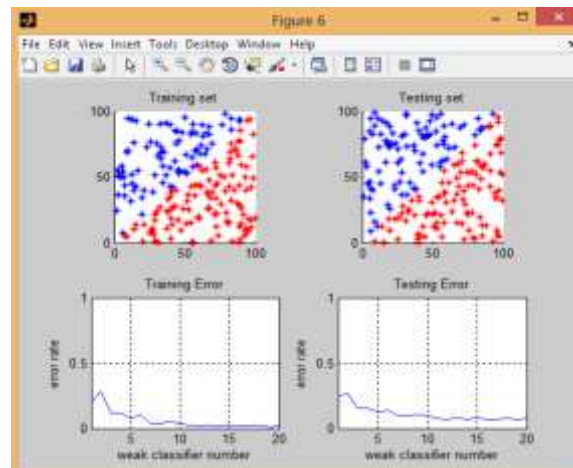
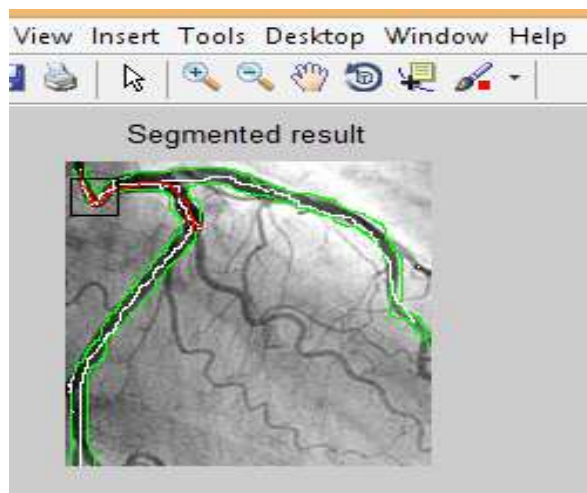


Fig 14: Error Rate in Classifier Segmentation (Graph Cut Algorithm)

4762





**Fig 15: Centerline extraction and Catheter detection**

**Comparative Statement**

Centerline extraction and catheter detection is done by using graph-cut algorithm and Gabor filters. The parameters such as entropy, standard deviation and time are compared with both filters is shown in table 2.

| Parameters         | By using Gaussian Filter | By using Gabor Filter |
|--------------------|--------------------------|-----------------------|
| Input image        |                          |                       |
| Output Image       |                          |                       |
| Entropy            | 0.7068                   | 0.4128                |
| Standard Deviation | 0.1916                   | 0.0501                |
| Elapsed time       | 12.64 sec                | 0.4422 sec            |

**Table 2: Comparative of filters**

**Conclusion**

Segmentation of coronary arteries in angiographic images is a fundamental tool to evaluate arterial diseases and choose proper coronary treatment. An accurate segmentation of coronary artery allows the physician to access different medical imaging information. Segmentation of vessels in angiographic images is done by Graph cut algorithm on analysis of vessel appearance „local connectivity to other vessels(Geodesic distance) and edgeness detection by canny edge detection algorithm. The interventional tool to remove blockages is catheter. Catheter can be of detected using point wise classification method using adaboost classifier. The same is done by using Gabor filter instead of Gaussian filter. It is found that time consumption is less and accuracy is more in Gabor filter techniques.

**Reference**

[1] W. E. Higgins, W. J. T. Spyra, E. L. Ritman, Y. Kim, and F. A. Spelman, "Automatic extraction of the arterial tree from 3-d angiograms", in IEEE Conf. Eng. in Medicine and Bio., vol. 2, pp. 563–564, 1989.

[2] N. Niki, Y. Kawata, H. Sato, and T. Kumazaki, "3d imaging of blood vessels using x-ray rotational angiographic system", IEEE Med. Imaging Conf., vol. 3, pp. 1873–1877, 1993.

[3] C. Molina, G. Prause, P. Radeva, and M. Sonka, "3-d catheter path reconstruction from biplane angiograms", in SPIE, vol. 3338, pp. 504–512, 1998.

[4] A. Klein, T.K. Egglin, J.S. Pollak, F. Lee, and A. Amini, "Identifying vascular features with orientation specific filters and b-spline snakes", in IEEE Computers in Cardiology, pp. 113–116, 1994.

[5] Karthick.S & Sathiyasekar.K, Performance Identification Using Morphological Approach on Digital Mammographic Images Current Signal Transduction Therapy, 2016, 11, 2 63-70.

[6] Dehkordi M T, Hoseini A M D, Sadri S, et al. Local feature fitting active contour for



segmenting vessels in angiograms[J]. IET Computer Vision, 2013, 8(3): 161--170.

[7] M'hiri F, Duong L, Desrosiers C, et al. Vesselwalker: Coronary arteries segmentation using random walks and hessian-based vesselness filter[C]//Biomedical Imaging (ISBI), 2013 IEEE 10th International Symposium on. IEEE, 2013: 918--921.

[8] Vos T, Allen C, Arora M, Barber RM, Bhutta ZA, Brown A, Carter A, Casey DC, Charlson FJ, Chen AZ, et al. Global, regional, and national incidence, prevalence, and years lived with disability for 310 diseases and injuries, 1990–2015: a systematic analysis for the global burden of disease study 2015. *Lancet*. 2016;388(10053):1545–602.

[9] Zhang H, Mu L, Hu S, Nallamothu BK, Lansky AJ, Xu B, Bouras G, Cohen DJ, Spertus JA, Masoudi FA, et al. Comparison of physician visual assessment with quantitative coronary angiography in assessment of stenosis severity in china. *JAMA Intern Med*. 2018;178(2):239–47.

[10] Mustafa W A, Mahmud A S, Aihsan M Z, Saifizi M and Charin C 2019 A Comparative Study of Different Blood Vessel Detection on Retinal Images *Int. J. Integr. Eng.* 11 231–6

[11] Zhao Y, Zheng Y, Liu Y, Zhao Y, Luo L, Yang S, et al. Automatic 2-D/3-D Vessel Enhancement in Multiple Modality Images Using a Weighted Symmetry Filter. *IEEE Trans Med Imaging*. 2018;37(2):438–50.

[12] Karthick.S & Sathiyasekar.K, Image Processing Method To Measure The Severity of Fungi Caused Disease In Leaf *International Journal of Advanced Research*, 2014, 2, 2, 95-100.

[13] Navab N, Hornegger J, Wells WM, Frangi AF. Structural Edge Detection for Cardiovascular Modeling. *Lect Notes Comput Sci (including Subser Lect Notes Artif Intell Lect Notes Bioinformatics)*. 2015;9351:735–42.

[14] Ajam A, Aziz AA, Asirvadam VS, Muda AS, Faye I, Safdar Gardezi SJ. A Review on Segmentation and Modeling of Cerebral Vasculature for Surgical Planning. *IEEE Access*. 2017;5:15222–40.

[15] Murayama Y, Fujimura S, Suzuki T, Takao H. Computational fluid dynamics as a risk assessment tool for aneurysm rupture. *Neurosurg Focus*. 2019;47(1).

[16] Ostrom QT, et al. Alex’s Lemonade Stand Foundation Infant and Childhood Primary Brain and Central Nervous System tumors diagnosed in the United States in 2007–2011. *Neuro-Oncology*. 2015;16(110):1–36.

[17] Drevelegas A, Papanikolaou N. Imaging modalities in brain tumors. In: Antonios D, editor. *Imaging of brain tumors with histological correlations*. Springer Berlin Heidelberg; 2011. p. 13-33.

[18] F. Gibou and R. Fedkiw, “A fast hybrid k-means level set algorithm for segmentation,” in 4th Annual Hawaii International Conference on Statistics and Mathematics, 2005, pp. 281–291.

[19] Louis DN, et al. The 2016 World Health Organization classification of tumors of the central nervous system: a summary. *Acta Neuropathol*. 2016;131(6):803–20.

[20] Karthick.S & Sathiyasekar.K, 2014, “A Survey on Hard Exudates Detection and Segmentation”, *International Journal of Scientific Engineering and Technology*, Volume No.3 Issue No.2, Pages: 154 – 158.

[21] A. Chakraborty, M. Worring, and J. S. Duncan, “On multifeature integration for deformable boundary finding,” in *Proc. Intl. Conf. on Computer Vision*, 1995, pp. 846–851.

[22] Karthick.S & Sathiyasekar.K, 2014, “A Research Review on Different Data Hiding Techniques”, *International Journal of Engineering and Computer Science*, Volume 3 Issue 1, Pages. 3655-3659.

[23] Tohka J. Partial volume effect modeling for segmentation and tissue classification of brain magnetic resonance images: A review. *World J Radiol*. 2014;6(11):855-64.

[24] Wen Z, et al. MR imaging of high-grade brain tumors using endogenous protein and peptide-based contrast. *Neuroimage*. 2010;51(2):616–22.



[25] S.Karthikeyan, Dr.M.Ezhilarasi, "Automatic Stroke Lesion Segmentation From Diffusion Weighted MRI Images" International Journal of Advanced Engineering Technology. Int J Adv Engg Tech/Vol. VII/Issue II/April-June, 2016/111-115 .

